ISSN 1674-1056
http://cpb.iphy.ac.cn
http://iopscience.iop.org/cpb
中国物理 B
Chinese Physics
中国物理 Chinese Physics B

Omnidirectional and compact Tamm phonon-polaritons enhanced mid-infrared absorber

Xiaomin Hua(花小敏), Gaige Zheng(郑改革), Fenglin Xian(咸冯林), Dongdong Xu(徐董董), and Shengyao Wang(王升耀)

Citation: Chin. Phys. B, 2021, 30 (**8**): 084202. DOI: 10.1088/1674-1056/abe22b
Journal homepage: http://cpb.iphy.ac.cn; http://iopscience.iop.org/cpb

What follows is a list of articles you may be interested in

Solar energy full-spectrum perfect absorption and efficient photo-thermal generation

Zhefu Liao(廖喆夫), Zhengqi Liu(刘正奇), Qizhao Wu(吴起兆), Xiaoshan Liu(刘晓山), Xuefeng Zhan(詹学峰), Gaorong Zeng(曾高荣), and Guiqiang Liu(刘桂强)
Chin. Phys. B, 2021, 30 (**8**): 084206. DOI: 10.1088/1674-1056/ac0696

Actively tunable polarization-sensitive multiband absorber based on graphene

Ai-Li Cao(曹爱利), Kun Zhang(张昆), Jia-Rui Zhang(张佳瑞), Yan Liu(刘燕), and Wei-Jin Kong(孔伟金)
Chin. Phys. B, 2020, 29 (**11**): 114205. DOI: 10.1088/1674-1056/abb663

Ultra wide sensing range plasmonic refractive index sensor based on nano-array with rhombus particles

Jiankai Zhu(朱剑凯), Xiangxian Wang(王向贤), Xiaoxiong Wu(吴枭雄), Yingwen Su(苏盈文), Yueqi Xu(徐月奇), Yunping Qi(祁云平), Liping Zhang(张丽萍), and Hua Yang(杨华)$
Chin. Phys. B, 2020, 29 (**11**): 114204. DOI: 10.1088/1674-1056/abb229

Broadband visible light absorber based on ultrathin semiconductor nanostructures

Lin-Jin Huang(黄林锦), Jia-Qi Li(李嘉麒), Man-Yi Lu(卢漫仪), Yan-Quan Chen(陈彦权), Hong-Ji Zhu(朱宏基), Hai-Ying Liu(刘海英)
Chin. Phys. B, 2020, 29 (**1**): 014201. DOI: 10.1088/1674-1056/ab5787

Nonlinear coherent perfect photon absorber in asymmetrical atom-nanowires coupling system

Xiuwen Xia(夏秀文), Xinqin Zhang(张新琴), Jingping Xu(许静平), Mutian Cheng(程木田), Yaping Yang(羊亚平)
Chin. Phys. B, 2018, 27 (**11**): 114205. DOI: 10.1088/1674-1056/27/11/114205

Omnidirectional and compact Tamm phonon-polaritons enhanced mid-infrared absorber*

Xiaomin Hua(花小敏)[1], Gaige Zheng(郑改革)[1,2,†], Fenglin Xian(咸冯林)[1,‡], Dongdong Xu(徐董董)[1], and Shengyao Wang(王升耀)[1]

[1] *Jiangsu Key Laboratory for Optoelectronic Detection of Atmosphere and Ocean, School of Physics and Optoelectronic Engineering, Nanjing University of Information Science and Technology, Nanjing* 210044, *China*

[2] *Jiangsu Collaborative Innovation Center on Atmospheric Environment and Equipment Technology (CICAEET), Nanjing University of Information Science and Technology, Nanjing* 210044, *China*

(Received 27 December 2020; revised manuscript received 28 January 2021; accepted manuscript online 2 February 2021)

Narrow band mid-infrared (MIR) absorption is highly desired in thermal emitter and sensing applications. We theoretically demonstrate that the perfect absorption at infrared frequencies can be achieved and controlled around the surface phonon resonance frequency of silicon carbide (SiC). The photonic heterostructure is composed of a distributed Bragg reflector (DBR)/germanium (Ge) cavity/SiC on top of a Ge substrate. Full-wave simulation results illustrate that the Tamm phonon-polaritons electric field can locally concentrate between the Ge cavity and the SiC film, contributed to the improved light-phonon interactions with an enhancement of light absorption. The structure has planar geometry and does not require nano-patterning to achieve perfect absorption of both polarizations of the incident light in a wide range of incident angles. Their absorption lines are tunable via engineering of the photon band-structure of the dielectric photonic nanostructures to achieve reversal of the geometrical phase across the interface with the plasmonic absorber.

Keywords: perfect absorption, surface phonon polaritons, mid-infrared, distributed Bragg reflector

PACS: 42.60.Da, 42.70.Qs **DOI:** 10.1088/1674-1056/abe22b

1. Introduction

Tamm plasmon-polaritons (TPPs) are optical states that can occur in the energy band gap on a photonic crystal (PhC) surface. The stop band of the PhC resembles the energy band gap due to Bragg reflections in its periodic structure.[1,2] The TPP is a standing wave, which is an interference phenomenon created by two surface waves propagating in opposite directions.[3] An interesting property of TPPs is that they interact with propagating light at any polarization states and angle of incidence, thus removing the need for the external compensation of wavevector.[4] The optical Tamm state corresponds to a narrow-band resonance mode with a strong electromagnetic field localization at the heterostructure interface, which can be used to improve absorption characteristics, nonlinear Kerr effect, and optical sensing methods.[5–8]

Analogous to TPPs, Tamm phonon-polaritons (TPhPs) were first predicted for a crystalline SiC film on a PhC and the experimental observation of the TPhP effect was reported recently.[9] As the mid-infrared (MIR) spectral region holds great promise technological applications in which chemicals have distinctive absorption signatures useful for their identification in many fields such as healthcare, defense, and environmental protection, various methods to extend the ideas of TPPs to MIR spectral range have been demonstrated.[9–12] Among them, the coupling behavior between TPP and cavity modes attracts special attention.[13] Especially, the interest in nearly perfect light absorption surrounds plenty of important optoelectronic applications ranging from optical communications, biomedical imaging to night vision cameras, and so on.

The purpose here is to investigate a one-dimensional (1D) layered structure for resonant selective thermal emission by excitation TPhPs at the interface between a polar semiconductor and a Bragg reflector suitable for the MIR range. The TPhP structure is composed of an aperiodic multilayer stack of dielectric layers (Ge and ZnS)/Ge/SiC on top of a Ge substrate. By designing the coupling between surface modes and the incident wave, we analytically demonstrate enhanced absorptivity (i.e. emissivity) at the designed wavelength. The modeled and simulated TPP structures for the mid-IR spectral region yield a promising approach for integrated sensing applications.

2. Model and methods

Surface phonon polariton (SPhP) is a result of the coupling between electromagnetic modes (photons) and lattice vibrational modes (optical phonons) at the surface of polar materials. Within the frequency range between the transverse (ω_{TO}) and longitudinal (ω_{LO}) optical phonon frequencies (known as the reststrahlen band), the real part of the dielectric function of the SiC is negative.[14–16] Thus, SiC acts as a mirror in this frequency range, similar to a metal but it is less lossy. Multi-

*Project supported by the National Natural Science Foundation of Jiangsu Province, China (Grant Nos. BK20191396, BK20180784).

†Corresponding author. E-mail: jsnanophotonics@yahoo.com

‡Corresponding author. E-mail: xfl@nuist.edu.cn

© 2021 Chinese Physical Society and IOP Publishing Ltd

layer structures containing SiC can support evanescent waves, which are characterized by an imaginary wavevector component in the direction perpendicular to the surface (to be denoted as z direction), i.e., their dispersion curve lies outside of the light cone.

By Kirchhoff's law, the selective enhancement of the emittance leads to a selective enhancement of the absorbance when considering incoming radiation. The designed structure with perfect absorption property is depicted as schematics in Fig. 1(a). Figure 1(b) exhibits the cross-session view in x–z plane. The transverse magnetic (TM) wave is defined as the light source and is normally incident to the array in simulation unless clarified. In the simulation, the optical property of Ge is from Palik's optical constants handbook[17] and the optical properties of the ZnS is from the literature.[18] The wavelength-dependent permittivity of the SiC was modeled by the Drude–Lorentz model[14,16]

$$\varepsilon_{\mathrm{SiC}} = \varepsilon_{\infty}\frac{\omega^2-\omega_{\mathrm{LO}}^2+\mathrm{i}\gamma\omega}{\omega^2-\omega_{\mathrm{TO}}^2+\mathrm{i}\gamma\omega}, \tag{1}$$

where ω_{LO} and ω_{TO} represent the longitudinal and transverse optical phonon frequencies, chosen as 972 cm^{-1} and 796 cm^{-1}, respectively; ε_{∞} is set as the high frequency dielectric constant and γ is defined as the damping rate due to vibrational an harmonicity. In this work, ε_{∞} is chosen to be 3.75 cm^{-1} and γ is set as 6.5.

Using the rigorous coupled wave analysis (RCWA) method,[19–21] we calculate the reflectance R as well as the electric field distribution. As our samples did not show any transmission in the same wavelength range, nor is there any patterning to scatter the incident light, the absorption spectrum can be calculated by $A(\lambda) = 1 - R(\lambda)$, the dips in reflection can be attributed to absorption. By Kirchhoff's law, we have $A(\lambda,\theta) = \varepsilon(\lambda,\theta)$ at thermal equilibrium, where ε is the emissivity. This allows the simulation of thermal radiation indirectly by means of considering the reflection problem.

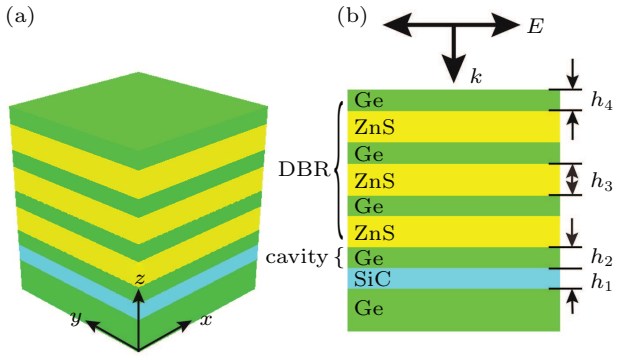


Fig. 1. (a) Schematic diagram and (b) cross-section view of the metamaterial absorber with DBR reflector.

3. Results and discussions

For determination, we investigate Ge with $h_4 = 0.75$ μm and ZnS with $h_3 = 1.25$ μm as materials of the alternating DBR layers. The absorption spectral under normal incidence with different numbers of layers (N) is shown in Fig. 2. Following the framework of Ref. [2], the electromagnetic field confinement inside a Tamm structure with a Bragg mirror and a metallic layer can be described as a two-mirror system. This structure can thus be seen as an optical cavity of null thickness, which means practically that the electromagnetic field will be confined over a small thickness localized at the Bragg-SiC interface. The resonance condition will then be achieved by introducing a thin layer of Ge between the SiC layer and the Bragg mirror.

We choose Ge and ZnS as the dielectric materials for the Bragg mirror as they are widely used in the MIR range for Bragg mirrors and other thin-layer structures and their deposition is well controlled. There is an optimized N for the realization of unity absorption. A narrow absorption peak can be observed at the wavelength of 12.34 μm, marked as I. The intensity of the absorption peak reduces to 82% with $N = 4$. The optical properties of the TPhP can be described using the temporal coupled mode theory.[22,23] With the increasing number of DBR pairs (N), the absorptance will slightly increase till six pairs of DBR for metal-side TPP structures, however, there is an optimal number of the DBR pairs for DBR-side TPP structures.

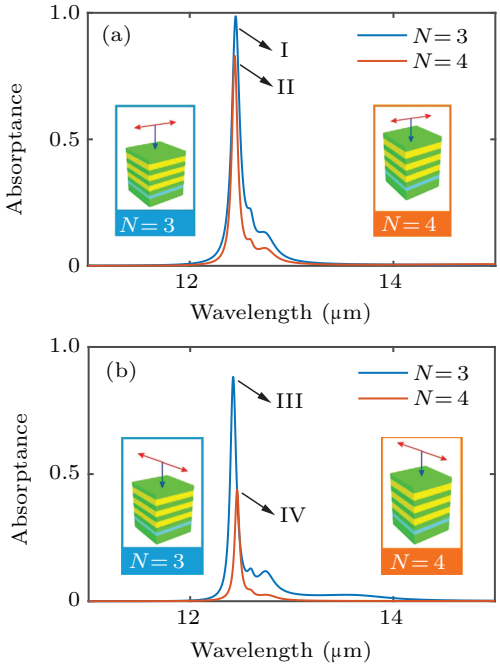


Fig. 2. Total absorption at normal incidence for (a) TM polarization and (b) TE polarization with the one-dimensional photonic crystal period number of 3 (blue line) and period number of 4 (orange line), respectively.

To further confirm the physical mechanism of resonances in absorber, the electric fields are quantitatively investigated and illustrated in Fig. 3. With the period number of 3, target resonance wavelength at 11.34 μm is shown in Fig. 3(a), the electric fields are significant confined into the interface SiC

and Ge cavity, which lead to a near unity absorption. To confirm the TPhPs, the optical field intensity $|E|^2$ can be divided by $|E_0|^2$, where E_0 is the incident electric field. The TPhP exhibits nearly a fifty-fold enhancement. Compared the electric field with the period number of 4, a week ability of structure to locate the energy of light which results in the low electric field strength in Fig. 3(b).

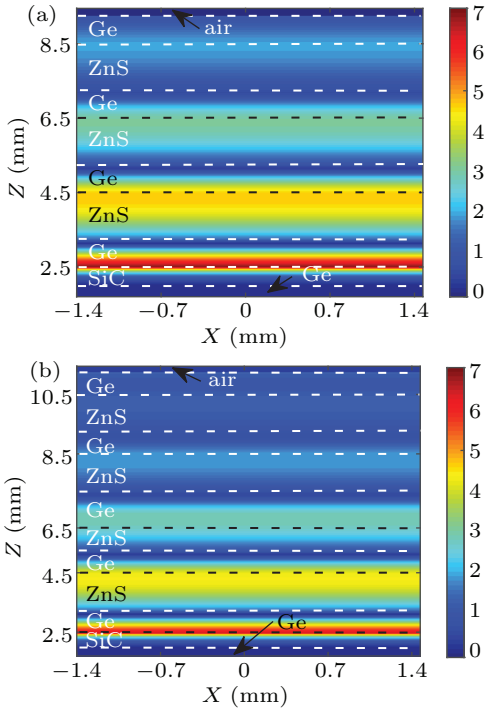


Fig. 3. (a) and (b) Electric field distribution profiles at the resonance wavelength of 11.34 μm in xz plane with three-layer one-dimensional photonic crystal and four-layer one-dimensional photonic crystal, respectively.

In the following study, the period number (N) is fixed at 3 to investigate the influences of the geometric parameters. In Figs. 4(a) and 4(b), the absorption spectra with various depth of Ge cavity has been exhibited, the absorption peak becomes of redshift when h_2 increases from 0.5 μm to 1 μm. From Fig. 4(b), we can see that h_2 has a considerable range for the modulation of the light absorption. The maximum appears when $h_2 = 0.8$ μm, where perfect absorption can be achieved. If an optical cavity is inserted between the DBR and the SiC film, the phase change of the light as it propagates one round trip in the cavity is equal to $2\pi^{2nh_2/\lambda}$. As a result, the resonance condition of the TP mode can be expressed as[24]

$$r_{\mathrm{DBR}} r_{\mathrm{SiC}}\, \mathrm{e}^{4\pi n h_2/\lambda} = 1, \tag{2}$$

where r_{DBR} is the reflection coefficient of a wave incident on the DBR from just after the SiC layer; r_{SiC} is the reflection coefficient of the wave incident on the SiC film from the DBR; and n represents the refractive index of Ge. The phase shift induced by the cavity thickness makes it possible to realize perfect absorption through changing the cavity thickness.

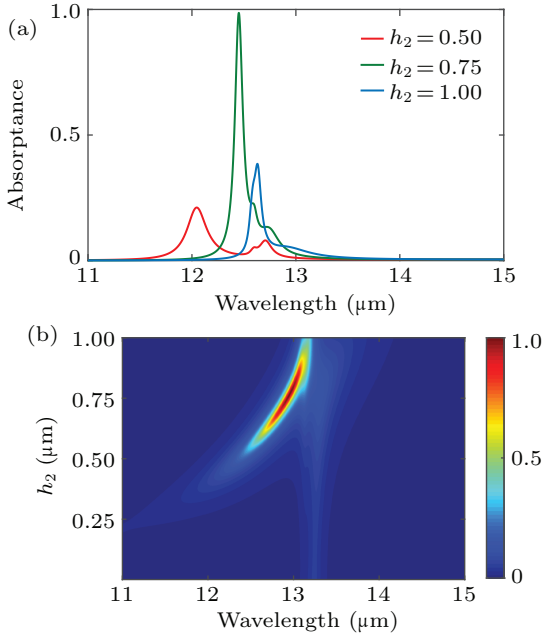


Fig. 4. (a) Simulated absorption spectra with different h_2. (b) Absorption map for various height of Ge cavity. The parameters are fixed as the same as used in Fig. 2.

In the following work, we study the dependences of absorption spectrum on h_1, h_3, and h_4. Based on these dependences, we further demonstrate the performance of the structure we designed. By studying the influence of the above parameters on the absorption spectrum, we choose optimal structural parameters to achieve perfect absorption. First, h_1 is changed to observe the change trend of the absorption spectrum as shown in Fig. 5(a). The absorption intensity is maintained from 0.3 μm to 0.8 μm, indicating a good manufacturing tolerance. Figure 5(b) shows the light absorption as a function of h_3. It can be seen that with increasing h_3, the position of the absorption peak is red-shifted, and the perfect absorption phenomenon will disappear. Figure 5(c) provides the simulated resonance wavelength as a function of h_4. As h_4 increases, the resonance frequency will red-shift to low frequency.

Angle stability is extremely important for MIR photodetectors, which is necessary to achieve a near unity absorption within a wide range of angles.[25–30] Therefore, we analyze the dependence of the absorption on the incident angle. The TPhP state can be excited by both TE and TM waves without a specific incident angle. As shown in Figs. 6(a)–6(d), regardless of the polarization, i.e., TE or TM, strong narrow band absorption can be maintained in various incident angles. According to Fig. 6, both of the absorption resonances observed at normal incidence are still present at higher angles of incidence. For incident angles over than 60°, more than 95% absorption is still can be obtained. Furthermore, the resonance does not shift significantly across the entire range of incident angles from 10° to 60°, nor is the resonance dependent on the polarization of the incident light.

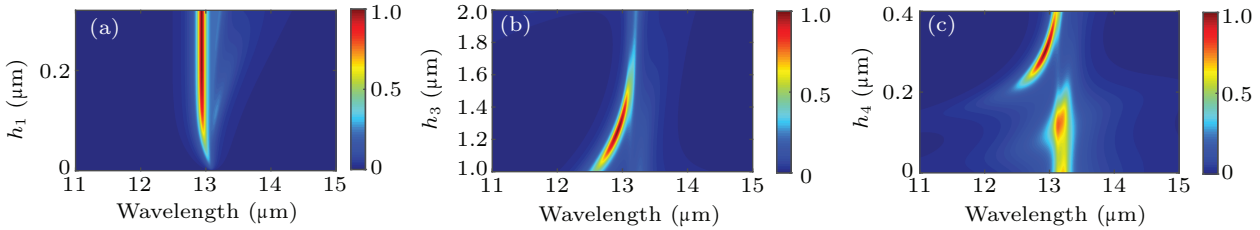


Fig. 5. Absorption map for various height of (a) SiC, (b) ZnS in DBR and (c) Ge in DBR, respectively. The DBR consists of three-layer one-dimensional photonic crystal and the parameters are fixed as the same as those used in Fig. 2.

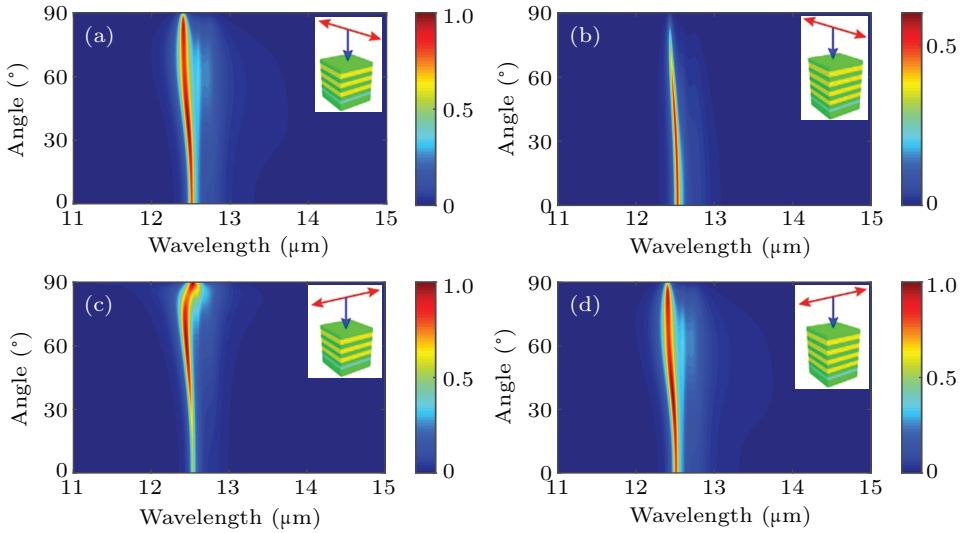


Fig. 6. Simulated absorption spectra with different angles of incidence, under the condition of (a) $N = 3$, TE polarization, (b) $N = 4$, TE polarization, (c) $N = 3$, TM polarization, (d) $N = 4$, TM polarization. The other parameters are fixed as the same as those used in Fig. 2.

4. Conclusions

In summary, we have proposed a photonic heterostructure composed of a distributed Bragg reflector (DBR)/germanium (Ge) cavity/SiC on top of a Ge substrate, which could effectively achieve the perfect absorption in the MIR region by taking advantage of the Tamm state and its local field enhancement characteristics. Spectrally selective perfect absorber is a specific application which requires both narrow band and wide-angle response. It has been shown that perfect absorption can be achieved when the angle of incidence is in the range of 0°–90° with suitable structural parameters. The effects of geometry parameters are also studied in detail. We hope that our design will find a potential application in optoelectronic devices where strong electromagnetic absorption is highly desired.

References

[1] Lu H, Li Y W, Yue Z J, Mao D and Zhao J L 2019 *APL Photon.* **4** 040801
[2] Kaliteevski M, Iorsh I, Brand S, Abram R A, Chamberlain J M, Kavokin A V and Shelykh I A 2007 *Phys. Rev. B* **76** 165415
[3] Vinogradov A P, Dorofeenko A V, Erokhin S G, Inoue M, Lisyansky A A, Merzlikin A M and Granovsky A B 2006 *Phys. Rev. B* **74** 045128
[4] Afinogenov B I, Bessonov V O, Nikulin A A and Fedyanin A A 2013 *Appl. Phys. Lett.* **103** 061112
[5] Wang J Y, Zhu Y S, Wang W H, Li Y Z, Gao R, Yu P, Xu H X and Wang Z M 2020 *Nanoscale* **12** 23945
[6] Lee K J, Wu J W and Kim K H 2013 *Opt. Express* **21** 28817
[7] Das R, Srivastava T and Jhac R 2015 *Sens. Actuators B* **206** 443
[8] Zhang W L, Wang F, Rao Y J and Jiang Y 2014 *Opt. Express* **22** 14524
[9] Juneau-Fecteau A, Savin R, Boucherif A and Fréchette L G 2019 *Appl. Phys. Lett.* **114** 141101
[10] Bao S and Zheng G G 2020 *Opt. Mater.* **109** 110307
[11] Pühringer G and Jakoby B 2018 *J. Opt. Soc. Am. B* **35** 1490
[12] Yang Z Y, Ishii S, Yokoyama T, Dao T T, Sun M G, Pankin P S, Timofeev I V, Nagao T and Chen K P 2017 *ACS Photon.* **4** 2212
[13] Silva J M S S and Vasilevskiy M I 2019 *Opt. Mater. Express* **9** 244
[14] Kiessling R, Tong Y J, Giles A J, Gewinner S, Schöllkopf W, Caldwell J D, Wolf M and Paarmann A 2019 *ACS Photon.* **6** 3017
[15] Li Y H, Qi R S, Shi R C, Li N and Gao P 2020 *Sci. Bull.* **65** 820
[16] Foteinopoulou S, Devarapu G C R, Subramania G S, Krishna D and Wasserman D 2019 *Nanophotonics* **8** 2129
[17] Palik and Edward D 1985 *Handbook of Optical Constants of Solids* (New York: Academic Press)
[18] Zhu H, Luo H, Li Q, Zhao D, Cai L, Du K, Xu Z, Ghosh P and Qiu M 2018 *Opt. Lett.* **43** 5230
[19] Zhang C, Wu K, Giannini V and Li X F 2017 *ACS Nano* **11** 1719
[20] Yu T, Zhang C, Liu H M, Liu J H, Li K, Qin L L, Wu S L and Li X F 2019 *Nanoscale* **11** 23182
[21] Li Q, Yu B Q, Li Z F, Wang X F, Zhang Z C and Pan L F 2017 *Chin. Phys. B* **26** 085202
[22] Lu H, Li Y W, Jiao H, Li Z W, Mao D and Zhao J L 2019 *Opt. Express* **27** 5383
[23] Hu J G, Yao E X, Xie W Q, Liu W, Li D M, Lu Y H and Zhan Q W 2019 *Opt. Express* **27** 18642
[24] Wang Z Y, Clark J K, Ho Y L, Vilquin B, Daiguji H and Delaunay J J 2018 *ACS Photon.* **5** 2446
[25] Chen C and Wang J 2017 *Chin. Phys. B* **26** 044101
[26] Chen X, Wu J H, Liu C R and Cao P 2019 *J. Opt. Soc. Am. B* **36** 153
[27] Li J S and Chen X S 2020 *Chin. Phys. B* **29** 078703
[28] Qin F, Chen X F, Yi Z, Yao W T, Yang H, Tang Y J, Yi Y, Li H L and Yie Y G 2020 *Solar Energy Mater. Solar Cells* **211** 110535
[29] Feng Y, Hu Z D, Balmakou A, Khakhomov S, Semchenko L and Wang J C 2020 *Plasmonics* **15** 1869
[30] Wang J C, Yang L, Wang M, Hu Z D, Deng Q, Nie Y G, Zhang F and Sang T 2019 *J. Phys. D: Appl. Phys.* **52** 015101